Article

De Novo Transcriptome Sequencing in Kiwifruit (*Actinidia chinensis* var. *deliciosa* (A Chev) Liang et Ferguson) and Development of Tissue-Specific Transcriptomic Resources

Juan Alfonso Salazar [1,*], Cristian Vergara-Pulgar [2,3], Claudia Jorquera [4], Patricio Zapata [4], David Ruiz [1], Pedro Martínez-Gómez [1], Rodrigo Infante [4] and Claudio Meneses [2,3]

1   Department of Plant Breeding, CEBAS-CSIC, P.O. Box 164, E-30100 Murcia, Espinardo, Spain; druiz@cebas.csic.es (D.R.); pmartinez@cebas.csic.es (P.M.-G.)
2   Centro de Biotecnología Vegetal, Facultad Ciencias Biológicas, Universidad Andrés Bello, República 217, Santiago 8370146, Chile; cvergarapulgar@gmail.com (C.V.-P.); claudio.meneses@unab.cl (C.M.)
3   FONDAP Center for Genome Regulation, República 217, Santiago 8370371, Chile
4   Departamento de Producción Agrícola, Universidad de Chile, Santiago 8820000, Chile; claudiajorquera@uchile.cl (C.J.); zapata.pzsm@gmail.com (P.Z.); rinfante@uchile.cl (R.I.)
*   Correspondence: jasalazar@cebas.csic.es

Abstract: Kiwifruit (*Actinidia chinensis* var. *deliciosa* (A Chev) Liang et Ferguson) is a sub-tropical vine species from the Actinidiaceae family native to China. This species has an allohexaploid genome (from diploid and autotetraploid parents), contained in 174 chromosomes producing a climacteric and fleshy fruit called kiwifruit. Currently, only a small body of transcriptomic and proteomic data are available for *A. chinensis* var. *deliciosa*. In this low molecular knowledge context, the main goal of this study is to construct a tissue-specific de novo transcriptome assembly, generating differential expression analysis among these specific tissues, to obtain new useful transcriptomic information for a better knowledge of vegetative, floral and fruit growth in this species. In this study, we have analyzed different whole transcriptomes from shoot, leaf, flower bud, flower and fruit at four development stages (7, 50, 120 and 160 days after flowering; DAF) in kiwifruit obtained through RNA-seq sequencing. The first version of the developed *A. chinensis* var. *deliciosa* de novo transcriptome contained 142,025 contigs ($\bar{x}$ = 1044 bp, N50 = 1133 bp). Annotation was performed with BLASTX against the TAIR10 protein database, and we found an annotation proportion of 35.6% (50,508), leaving 64.4% (91,517) of the contigs without annotation. These results represent a reference transcriptome for allohexaploid kiwifruit generating a database of *A. chinensis* var. *deliciosa* genes related to leaf, flower and fruit development. These results provided highly valuable information identifying over 20,000 exclusive genes including all tissue comparisons, which were associated with the proteins involved in different biological processes and molecular functions.

Keywords: *Actinidia*; breeding; de novo transcriptome; kiwifruit leaf; flower; fruit development

1. Introduction

Actinidia chinensis var. *deliciosa* is an allohexaploid species (2n = 6x) with an estimated genome size of 4.4 Gbp and 174 chromosomes [1–3]. It is a species that originated in southwestern China and belongs to the genus *Actinidia*, which includes at least 76 species [4]. This species has an important economic role due to its edible fruit known as kiwifruit, being also a species of nutritional importance due to its high level of vitamin C [5]. The kiwifruit worldwide production in 2019 reached about 4.35 million tons, China being the most important producer, followed by New Zealand, Italy, Iran, Greece and Chile. However, most of the Chinese kiwifruit are locally consumed, with less than 0.2% of the total being exported (http://faostat.fao.org (accessed on 4 January 2021)).

The *Actinidia* genus is mainly composed of dioecious plants. The flowers are axial with five petals, usually white colored, and sepals that can be fused with the base or not.

The fruit is a berry and has black seeds embedded within the flesh where the colors and morphology vary depending on the cultivar. *Actinidia chinensis* var. *deliciosa* cv. 'Hayward' is one of the most widely distributed cultivars, and bears fruits with green flesh and a fuzzy appearance. The characteristic flavor of the kiwifruit is one of the important aspects for consumer acceptance and its commercial potential. The balance of sweetness and acidity is given by the sugars such as glucose, fructose, sucrose and myo-inositol in small quantities, and the acids found in the mature fruit including quinic acid, citric acid and in less proportion, malic acid [6]. From a molecular point of view, at the genomic level, the whole-genome sequencing of the heterozygous 'Hongyang' cultivar [7] and the 'Red5' genotype [8] has been reported. In addition, at this moment the most recent works are those corresponding to the genome assembly of *Actinidia eriantha* [9], the high-quality *Actinidia chinensis* genome [10] and the current kiwifruit genome database [11], which will undoubtedly provide valuable information at the genomic level. However, the information at the transcriptomic, proteomic or metabolomic levels is scarcer, mainly in the case of important kiwi commercial cultivars such as 'Hayward' taking in account its ploidy level. Transcriptomic analyses are relatively recent in kiwifruit species, focused on physiology and fruit ripening studies or resistance to diseases. These transcriptomic studies included the sequencing of whole male and female transcriptomes of *A. arguta* flower buds [12], the study of fruit development in the cultivar "Hongyang" based on long noncoding RNA expression and alternative splicing [13], the premature bud break dormancy analysis [14], the genome-wide gene expression profiles in male and female plants using high-throughput RNA sequencing (RNA-seq) [15], or transcriptomic analysis studies about bacterial and fungal diseases such as *Pseudomonas syringae pv. actinidiae* (Psa) [16,17] and *Botryosphaeria dothidea*, which produce important losses in kiwifruit [18]. More recently, new studies have been focused on the study of post-harvest behavior after the application of ethylene-related phytohormones such as 1-MCP (ethylene inhibitor) and Ethrel (ethylene precursor), which provides more knowledge about the kiwifruit shelf-life extension [19]. In addition, some transcriptomic studies have been reported showing new findings on anthocyanin biosynthesis in *A. chinensis* [20,21] and *A. arguta* [22]. Finally, from the proteomic and metabolomic point of view, we can highlight the study in *Actinidia arguta* by using iTRAQ-based quantitative proteomic which is providing a new approach according to flesh development color in kiwifruit [23] or the current metabolomic study about *A. arguta* leaves with nutraceutical values [24]. All these transcriptomic, proteomic and metabolomic studies were focused on the specific areas that deal with the most important problems of kiwifruit and that suppose important agronomic and economic impact. According to plant tissue development at the physiological level, gibberellins are a large family of isoprenoid phytohormones which act as growth regulators in higher plants [25]. Thus, gibberellins stimulate cell elongation or cell division being involved in the seed germination, maturation or flowering of many vascular species [26]. The synthesis of these isoprenoids can be mediated by the mevalonate or methylerythritol phosphate pathways [25]. Therefore, the role of both of these pathways could be an interesting approach in order to discern the mechanisms involved in the tissue-specific development process.

The objective of this work was the development of a de novo transcriptome in green-fleshed kiwifruit 'Hayward' using RNA-seq analysis from the leaf, flower and fruit tissues in different development phases, including a differential gene expression analysis to generate a database of genes related to the leaf, flower and fruit development and to identify the most important proteins involved in these development processes. Additionally, the most important kiwifruit genes linked to these processes were identified, illustrating the powerfulness and usefulness of this transcriptomic resource.

2. Materials and Methods

2.1. Plant Material and RNA Sequencing

Sample tissues of *Actinidia chinensis* var. *deliciosa* cv. 'Hayward' including shoots, leaves, flower buds, flowers and fruits at 7, 50, 120 and 160 days after full bloom (DAFB)

(Figure 1) were collected and immediately frozen in liquid nitrogen from the Germán Greve Silva experimental station in Rinconada de Maipú (University of Chile). 'Hayward' flowers were pollinated using pollen from 'Belen' variety. RNA was extracted from three biological replicates using the RNeasy Mini Kit (Qiagen®, Hilden, Germany). To verify sample integrity, total RNA was evaluated on Fragment Analyzer™ Automated CE System (AATI) and quantified by Qubit® 2.0 Fluorometer, using Qubit™ RNA BR Assay Kit (Life Technologies, Carlsbad, CA, USA). For library construction, one microgram of RNA sample was used as input for Illumina® TruSeq RNA HT Sample Prep Kit, according to the manufacturer's instructions. Final libraries were analyzed on an NGS kit for Fragment Analyzer™, and quantified by Qubit® 2.0 Fluorometer, using Qubit™ DNA BR Assay Kit. Libraries were sequenced on HiSeq 2500 platform (Illumina Inc., San Diego, CA, USA).
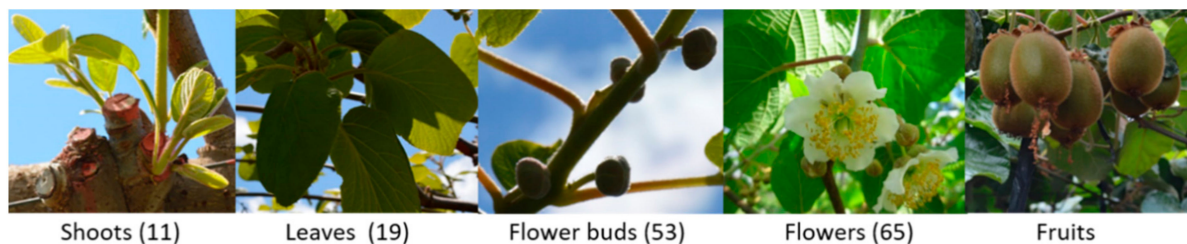

Figure 1. Tissues assayed in kiwifruit cv 'Hayward' including shoots leaves unfolded (11), leaves completely developed (19), flower buds growing (53), full flowering (65), fruits as the following days after full bloom (DAFB): 7, 50, 120 and 160 days. Between parenthesis are indicted the phenological stage References [27].

2.2. Transcriptome Assembly and Refining

Total reads were analyzed (pre- and post-trimming) and trimmed with FastQC software and FLEXBAR software (https://github.com/seqan/flexbar (accessed on 5 October 2020)) in order to filter low-quality reads (Phred score less than 25) and remove reads either short or with Ns in the sequence. Remaining reads after trimming were used as input in the transcriptome assembly using Trinity software (https://github.com/trinityrnaseq (accessed on 5 October 2020)). The refinement of the transcriptome was made using CD-HIT (http://weizhongli-lab.org/cd-hit/ (accessed on 5 October 2020)) to remove duplicate contigs with a 0.9 identity setting and Corset (https://github.com/Oshlack/Corset/wiki (accessed on 5 October 2020)) to filter out contigs with less than 30 reads mapping to each contig in the assembly.

2.3. Assessment of Assembly Metric, Quality and Annotation

Transcriptome metric measurement was performed by TrinityStats.pl Software, a quality assessment was performed by two ultra-conserved protein gene finder softwares (CEGMA and BUSCO; http://korflab.ucdavis.edu/datasets/cegma/ (accessed on 5 October 2020); http://busco.ezlab.org/ (accessed on 5 October 2020)). Annotation was performed with DIAMOND, (https://github.com/bbuchfink/diamond (accessed on 5 October 2020)) in BLASTX mode against TAIR10 protein database, reporting hits with minimum e-value of 0.001. To explore the main gene functions involved in the vegetative growth leaves, floral and fruit development from the biological processes and molecular function point of view we performed a singular enrichment analysis (SEA) by Panther G0 slim [28] and AgriGo v2 [29], using the top hit species *Vitis vinifera* as reference.

2.4. Principal Component Analysis and Sample Similarity

A principal component analysis (PCA) was conducted to evaluate in a non-supervised way, the grouping and similarity of each sample and corresponding biological replicates, along with a sample similarity heatmap. Both graphs were constructed with the R-based PtR script ("–log2 –CPM –center_rows –prin_comp 3" parameters) from Trinity analysis

utilities using the counts matrix containing every sample and its replicates as an input. For sample similarity, Spearman's correlation coefficient was used.

2.5. Differential Expression Analysis and Protein-Protein Interaction Network

Raw counts of each contig were obtained with RSEM (https://deweylab.github.io/RSEM/ (accessed on 5 October 2020)) using Bowtie2 aligner (http://bowtie-bio.sourceforge.net/bowtie2/index.shtml (accessed on 5 October 2020)) to align all the input reads to the de novo assembled transcriptome. Then all counts and replicates per tissue were used to develop a raw counts' matrix. From this raw count, a TPM–TMM normalized matrix was calculated and used for the study alongside the raw counts' matrix. Differential expression analysis was performed by using the R's package edgeR from Bioconductor (http://bioconductor.org/packages/release/bioc/html/edgeR.html (accessed on 5 October 2020)). Differentially expressed genes (DEGs) were used for further comparisons and downstream analyses. Finally, a protein–protein interaction network was developed in order to associate DEGs with metabolic processes by using the STRING database [30], considering a score >0.400 for the assayed DEGs.

3. Results

3.1. Refined De Novo Transcriptome Assembly

In order to obtain a multiple-tissue de novo transcriptome of genes from *Actinidia chinensis* var. *deliciosa*, RNA libraries were constructed and sequenced from the shoots, leaves, flower buds, flowers and fruits at 7, 50, 120 and 160 DAFB with a total of 604,735,364 pair-end reads (150 bp × 2) (Table S1a). All the raw reads in the FastQ format, including the pair-end and replicates, are available from the NCBI Short Read Archive (SRA) database under the bioproject number PRJNA564374 (https://www.ncbi.nlm.nih.gov/sra/PRJNA564374 (accessed on 5 October 2020)). These reads were processed and trimmed to remove any low-quality reads and then used as the input to assemble the transcriptome with the Trinity software. The assembled and refined transcriptome contains 142,025 total contigs, where 106,603 contigs are trinity "genes" unigenes. Moreover, the average size for the contigs was 1044, the largest one reaching 36,186 bp while the shortest was 501 bp long (Table 1 and Table S1b).

Table 1. Summary of the de novo transcriptome metrics and annotation summary.

Metric	
Total Contigs	142,025
Trinity "Genes"	106,630
Average contig (bp)	1,044
[1] CEGMA Score (%)	C: 56.8; F: 35.1; M: 8.1
[2] BUSCO Score (%)	C: 69.9; F: 18.3; M: 11.8

[1] CEGMA dataset used contains 248 eukaryotic proteins. C: complete genes found from the dataset, F: fragmented genes found from the dataset, and M: missing genes. [2] BUSCO dataset used contains 1440 plant-specific proteins. C: complete genes found from the dataset, F: fragmented genes found from the dataset, and M: missing genes.

In addition, to assess the quality for our de novo transcriptome, we performed a biological-based analysis approach. The biological analysis needs the use of the ultra-conserved proteins encoded in the assembled transcriptome, searching them and reporting how many are completed, fragmented and missing. We used CEGMA and BUSCO to evaluate the completeness of the ultra-conserved protein coding genes for the eukaryote and plant species. CEGMA found 140 (56.8%) complete, 87 (35.1%) fragmented and 20 (8.1%) missing genes from its 248 eukaryotic ultra-conserved protein data set. However, BUSCO found 1007 (69.9%) complete, 263 (18.3%) fragmented and 170 (11.8%) missing genes from the ultra-conserved plant database (1440 total plant-specific proteins) (Table 1). Finally, an additional quality control of the samples and biological replicates was performed

using Trinity's auxiliary scripts (Figure 2), showing high similarities between the biological replicates and variable differences among the different tissues samples.
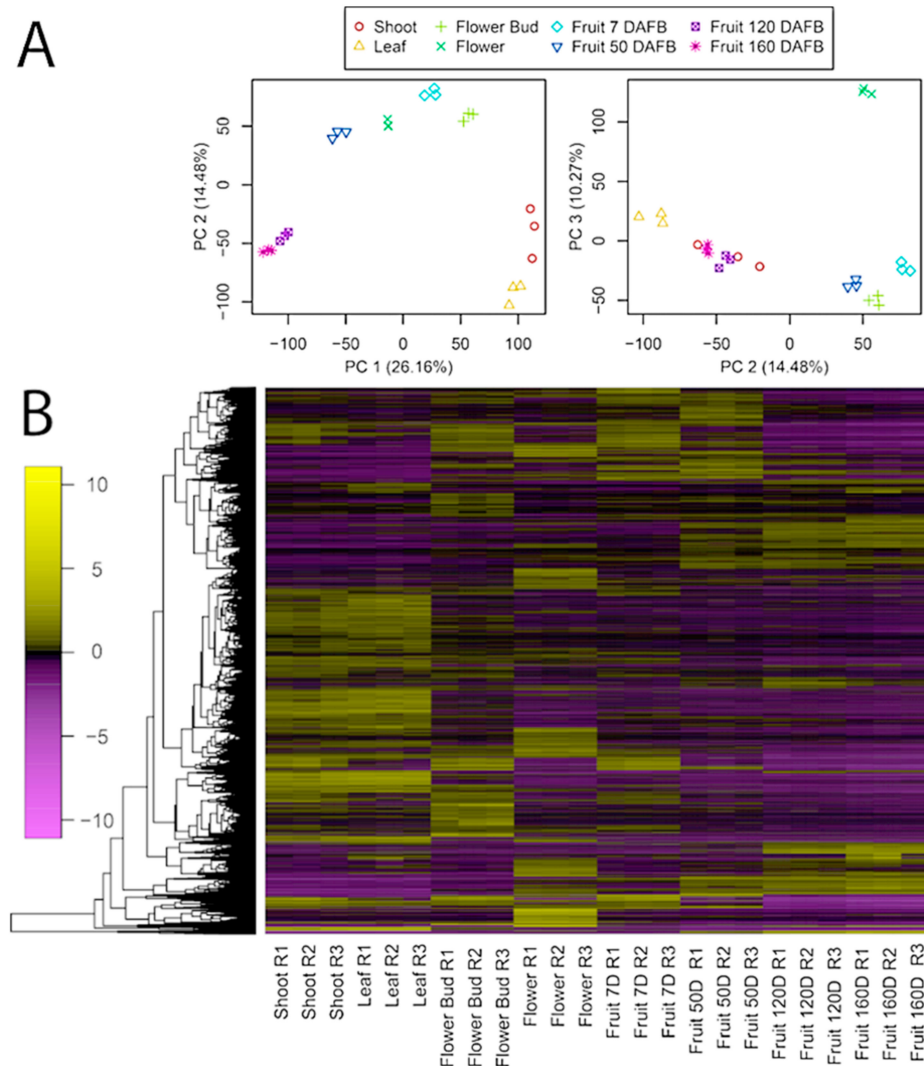

Figure 2. (**A**) Principal component analysis (PCA) of the four development stages of the study and its biological replicates (R). In the Y-axis is the principal component (PC) 2 and 3 and in the X-axis is the principal component 1 and 2, respectively. (**B**) Heatmap with filters of fold change ≥ 4 and FDR 0.05 across all tissues and replicates. Y-axis represents the genes while the X-axis shows all sample tissues and replicates. The color key represents the median centered log2 TMM-normalized TPM values. Yellow indicates a high level of expression, black indicates no change in expression, and purple indicates a low level of expression.

3.2. Gene Annotation and Enrichment Analysis

The main gene functions involved in the vegetative growth of the leaves, and the floral and fruit development were analyzed from the biological processes and molecular function point of view, using the top-hit species *Vitis vinifera* as the reference (Figure 3; Figures S1–S9; Tables S2 and S3). According to the annotations by Panther (Table S2) in shoot vs. leaf comparisons for the biological processes, the top hits GO terms were metabolic processes (23.1%; GO:0008152) and cellular component organization or biogenesis (23.1%; GO:0071840), while for molecular function it was molecule binding (42.9%; GO:0005488). As for flower bud vs. flower, the most important GO term for the biological processes were metabolic processes (45.9%; GO:0008152), while for molecular function it was the catalytic activity (45.1%; GO:0003824) as well as for fruit development (fruit7 d vs.

50 d–120 d–160 d) the top hits for the biological processes and molecular function were also metabolic processes (45.7%; GO:0008152) and catalytic activity (51.8%; GO:0003824), respectively.
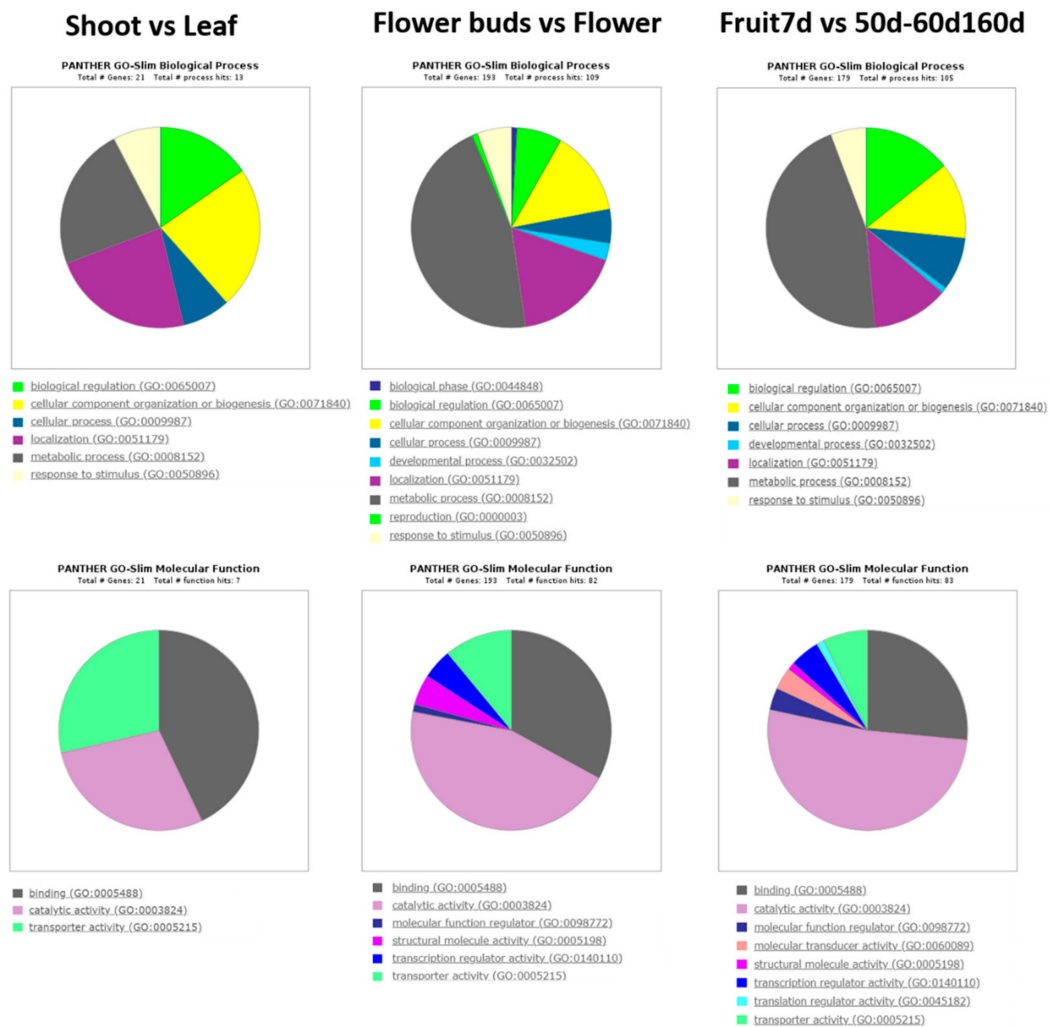

Figure 3. Panther GO annotations for each comparative plant tissues shoot vs. leaf, flower bud vs. flower and fruit7 d vs. 50 d–120 d–160 d (including all fruit tissues together).

In the GO analysis by using AgriGO v2 (Table S3), only eight GO terms were found for shoot vs. leaf according to the *p*-value, thus we can highlight the response to the stimulus (1.3e-04; GO:0050896) and nucleic-acid binding (1.8e-05; GO:0003676) for the biological processes and molecular function, respectively. According to floral and fruit development, we found 119 and 56 GO terms, respectively. A total of 69 GO terms were exclusives for flower bud vs. flower while only six were exclusives for fruit7 d vs. 50 d–120 d–160 d (Table S3).

3.3. Transcriptome Annotation and Differential Expressed Genes

After the annotation process against the TAIR10 protein database, we obtained a total of 50,508 contigs (35.6%) annotated, leaving 91,517 contigs (64.4%) without annotations (Table 2; Table S2). From the annotated contigs, 99.99% corresponded to a diverse plant species. The top three hit species were *Vitis vinifera* (18.2%), *Juglans regia* (5.8%) and *Coffea canephora* (4.3%) (Table 2 and Table S4). Also, we found that 1.5% of the annotation corresponds to the *Actinidia* genus.

Table 2. Functional annotations and top-hit species summary.

Functional Annotation	
Total contigs annotated	50,508
Total contigs unannotated	91,517
Top-hit species (%)	
Vitis vinifera	18.2%
Juglans regia	5.8%
Coffea canephora	4.3%
Actinidia genus	1.5%

In order to perform a general comparison of the number of gene expression differences between the tissues, a differential expression analysis was performed. When comparing all the replicates and tissues (using a normalized factor based on the fold change between each expression and the mean expression across the samples) with filters of the false discovery rate (FDR) $\geq$ 0.005 and FC $\geq$ 4, we found around 49,000 differential expressed genes (Figure 2). In addition, to obtain a better understanding about the tissues comparison, differential gene expression was evaluated by edgeR [31], grouping different tissues as follow: shoot vs. leaf, flower bud vs. flower, fruit 7 d vs. fruit 50 d, fruit 7 d vs. fruit 120 d and fruit 7 d vs. fruit 160 d (Figure 4 and Figure S10). Thus, through these comparisons we can obtain the overexpressed and under expressed genes of each tissue comparison related to the leaves vegetative growth, and the flower and fruit development. Finally, we've obtained 22,962 exclusive genes for all the tissue comparisons at *p*-value < 0.001, obtaining 1567 (shoot vs. leaf), 10,634 (flower bud vs. flower), 2113 (fruit7 vs. 50), 3560 (fruit7 vs. 120) and 5088 (fruit7 vs. 160) (Figure 4; Table S4).
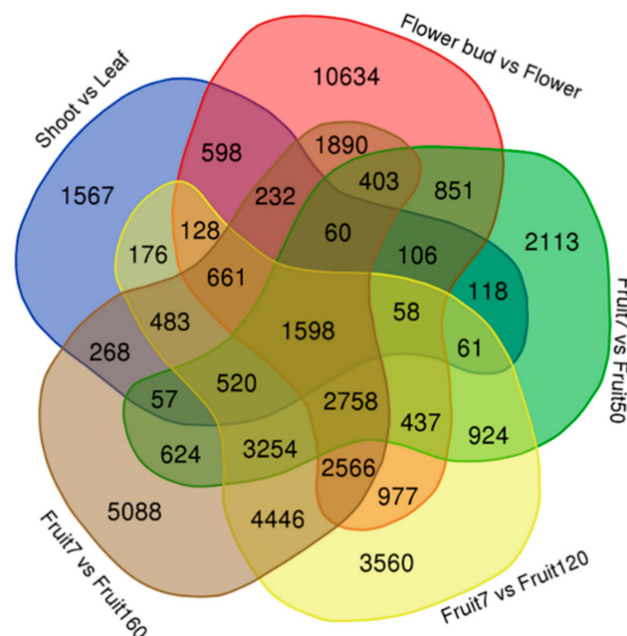

Figure 4. Venn diagram for differential expression genes between the following different plant tissues: shoot vs. leaf, flower bud vs. flower, fruit7 vs. fruit50, fruit7 vs. fruit120 and fruit7 vs. fruit160 at *p*-value < 0.001.

On the other hand, if we analyze each tissue separately, the highest number of expressed contigs was for flower bud vs. flower, the vegetative and fruit tissues being lower expressed. However, the number of expressed contigs increased with the fruit development time from 7 to 160 days (Figure 5A). If we compare up- and down-regulated contigs, the previous stage of each plant tissue comparison showed a lower number of up-regulated

contigs, except in the case of the fruit at 7 vs. 160 days where a higher number of up-regulated contigs for fruit at 7 vs. 160 days was appreciated (Figure 5B). This event was presumably due to the fact that fruits after 160 days reached their maximum development, giving a greater number of up regulated contigs in favor of day 7 contrary to day 160. A summary of the main genes involved in each tissue comparison is shown (Table S5), obtaining a total of 120 genes with a logFC over 2.
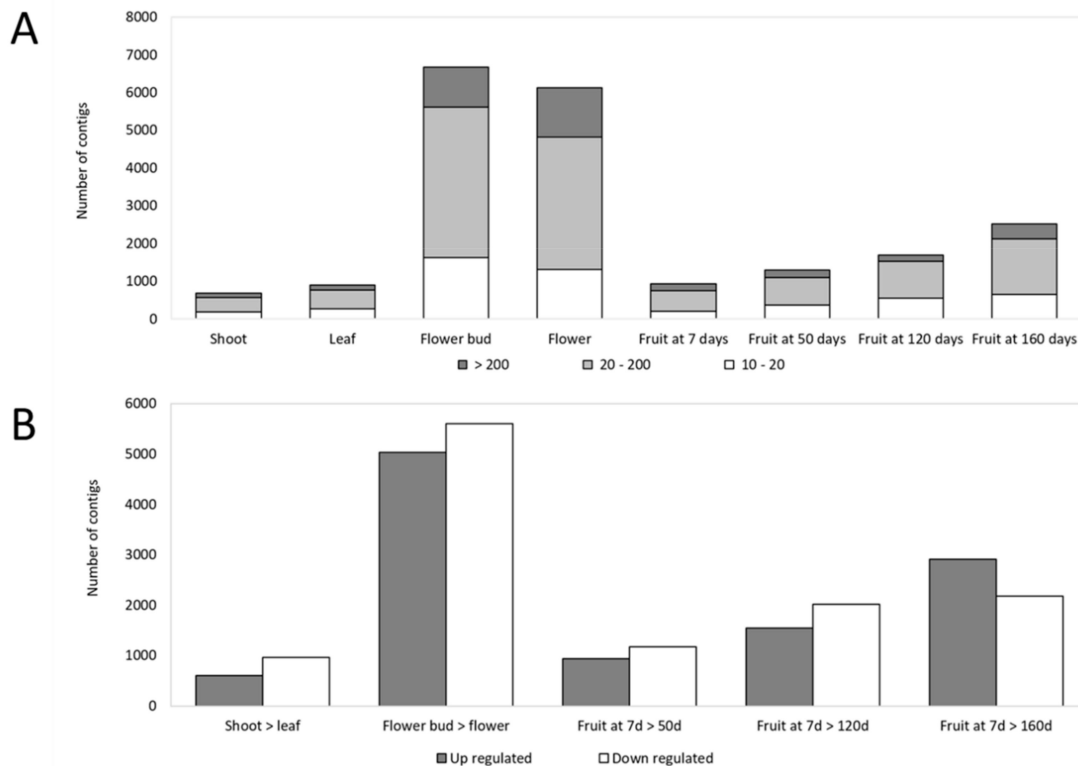

Figure 5. (**A**) Number of expressed contigs by plant tissue (above). Contig expression is shown in white color (10–20), grey (20–200) and dark grey (>200). (**B**) Number of expressed contigs by tissue comparison (below). Up-regulated (grey color) and down-regulated (white color) contigs.

If we pay attention to the most significant contigs according to the logFC over 2, some examples of DEGs were shown in the heatmap (Figure 6). As for shoot vs. leaf comparison, the protein KDP41561.1 (hypothetical protein JCGZ_15968 (*Jatropha curcas*)) was overexpressed in the shoots while the protein XP_010651436.1 (type 2 DNA topoisomerase 6 subunit B-like isoform X1 (*Vitis vinifera*)) was overexpressed in the leaves. In addition, a contig linked to the protein ALO19891.1 (UDP-glycosyltransferase 84J2) (*Camellia sinensis*)) was overexpressed in the leaf (Table S5). According to flower bud vs. flower comparison, XP_002308583.2 (hypothetical protein POPTR_0006s24990g (*Populus trichocarpa*) and XP_010279585.1 (cytokinin dehydrogenase 9-like) (*Nelumbo nucifera*) were overexpressed in the flower buds and flower, respectively (Table S6). As for the fruit comparison between fruit 7 d vs. fruit 120 d, we can highlight XP_010924477.1 (probable inositol oxygenase (*Elaeis guineensis*)), which was overexpressed in fruit 120 d while in the comparison between fruit 7 d and fruit 160 d XP_016207777.1 (calcium-binding protein CML39 (*Arachis ipaensis*)) as well as XP_010654040.1 (heat stress transcription factor A-2e isoform X2 (*Vitis vinifera*)) were both overexpressed in fruit 160d (Table S5).
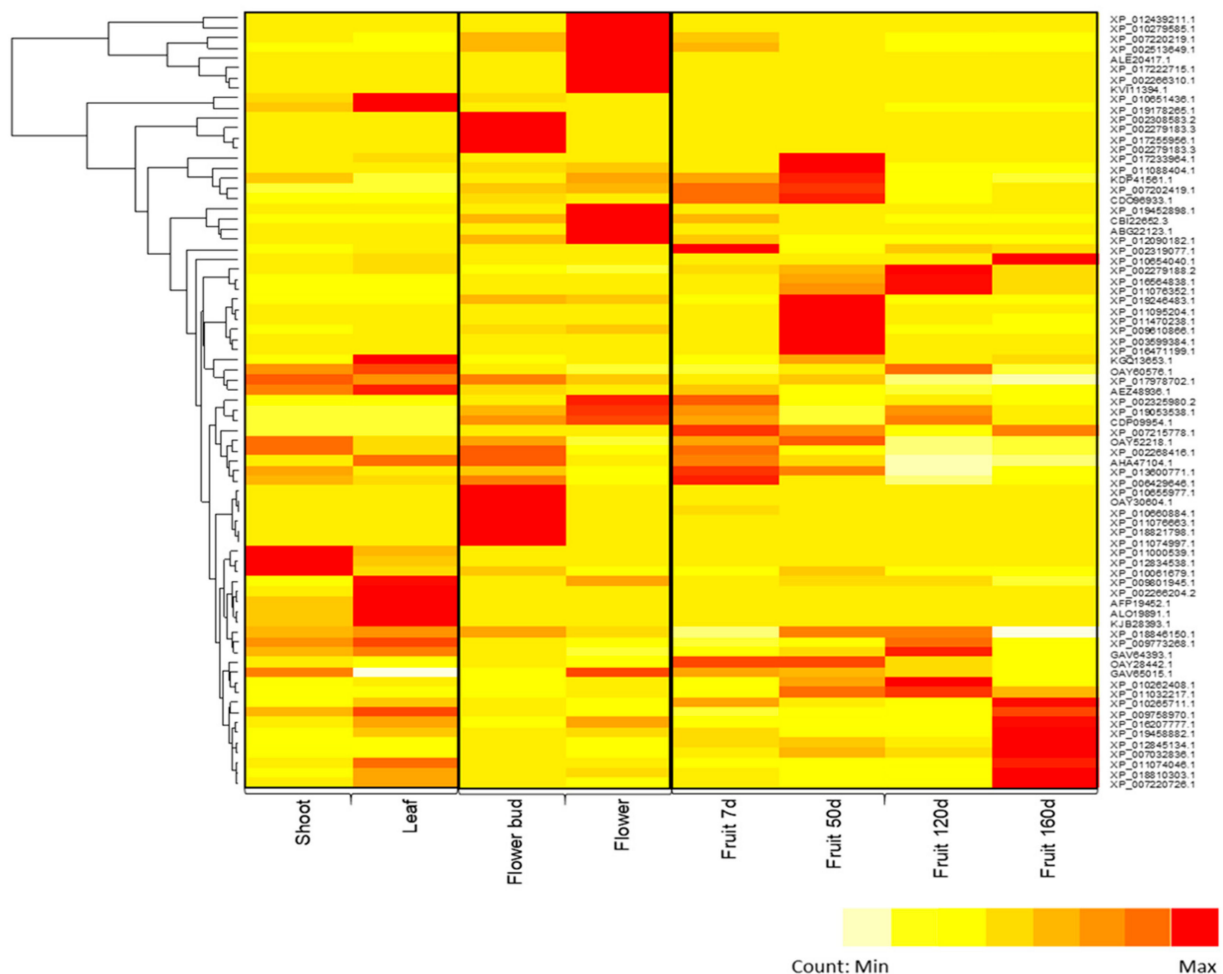
Figure 6. Summary of the top-hit genes up- and down-regulated considering shoot, leaf and fruit tissues (d7, d50, d120 and d160). Light yellow color indicates a minimum value of counts while red indicates a maximum count.

3.4. Protein–Protein Interaction Network

According to the protein–protein interaction, protein IDs from *Vitis* matched with our *Actinidia* contigs were used in the STRING tool for each plant tissue comparison. When we analyzed the shoot vs. leaf, we observed three clusters differentially expressed related to the plant circadian rhythm, RNA transport and a third cluster mainly related to the sulfur and nitrogen metabolism involved in specific tissue differentiation (Figure 7 and Table S6).

In the comparison between the flower buds and flowers, two main protein clusters were shown. The biosynthesis of secondary metabolites, phenylpropanoid biosynthesis, or cysteine and methionine metabolism were the main routes involved. The enzyme mevalonate kinase (VIT_14s0128g00330.t01) is, however, the unique protein that connects both the clusters, and for this reason this enzyme could be one of the keys involved in the flower development process (Figure 8 and Table S6).
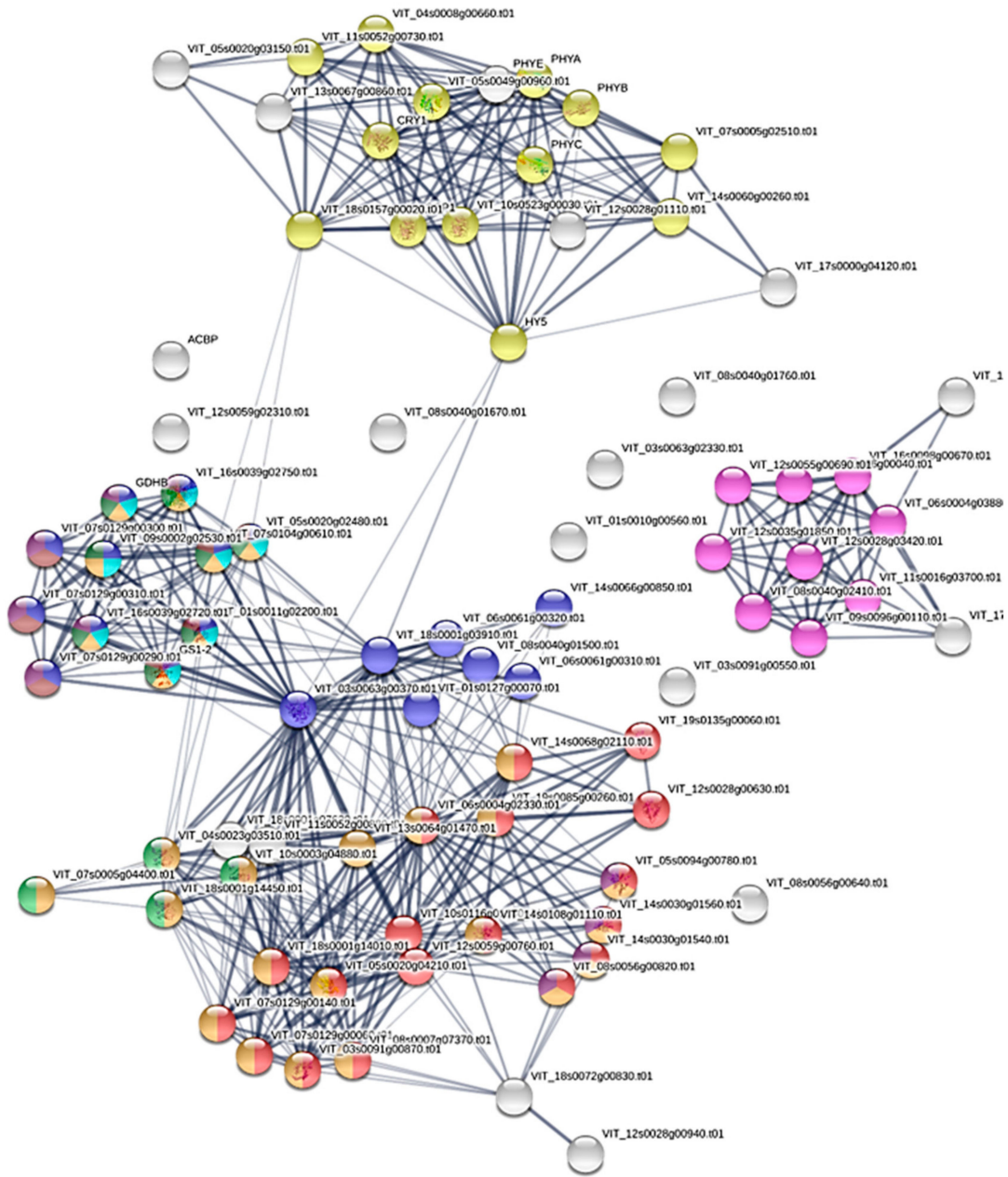
Term ID	Term description	Gene	FDR	
vvi00920	Sulfur metabolism	18 of 33	6.37e-33	
vvi00910	Nitrogen metabolism	18 of 33	6.37e-33	
vvi04712	Circadian rhythm - plant	13 of 63	1.88e-19	
vvi00220	Arginine biosynthesis	8 of 29	4.63e-13	
vvi01100	Metabolic pathways	27 of 1867	2.04e-12	
vvi00250	Alanine, aspartate and glutamate metabolism	8 of 42	4.17e-12	
vvi03013	RNA transport	9 of 146	1.48e-09	
vvi00630	Glyoxylate and dicarboxylate metabolism	7 of 69	4.77e-09	
vvi01200	Carbon metabolism	10 of 243	5.02e-09	
vvi00195	Photosynthesis	4 of 55	3.18e-05	

Figure 7. Protein–protein interaction network for shoot vs. leaf comparison.

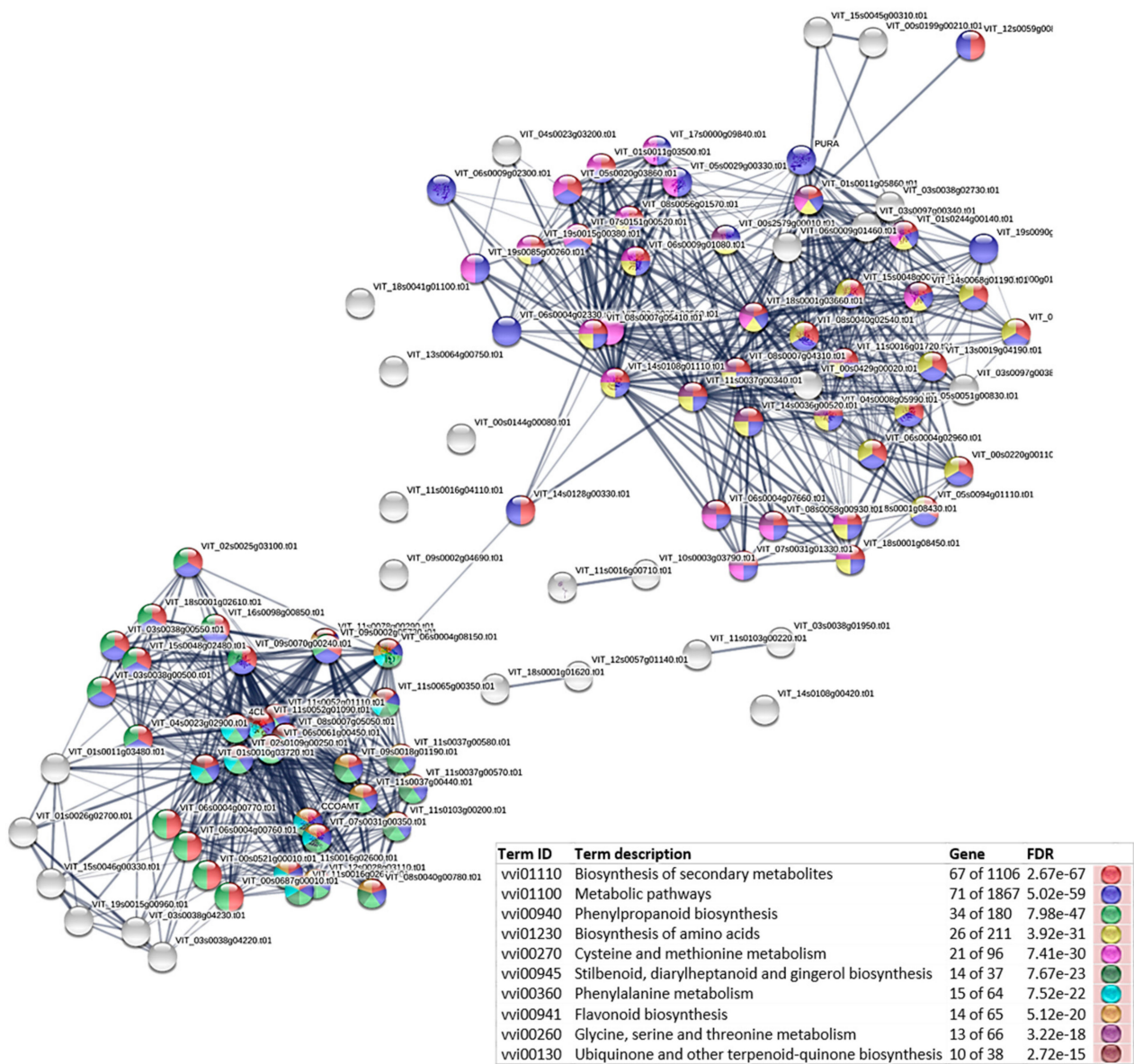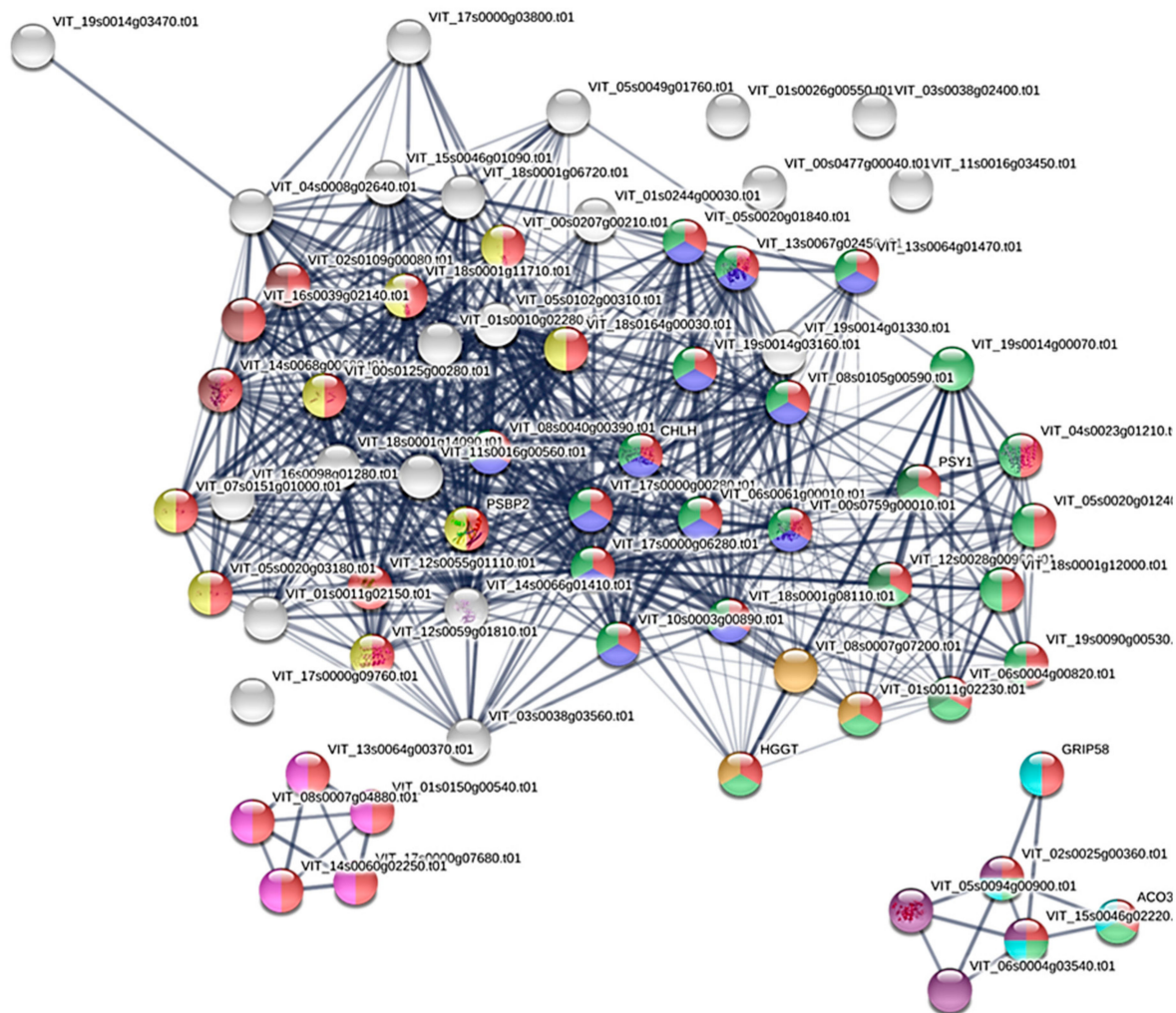| Term ID	Term description	Gene	FDR	
vvi01110	Biosynthesis of secondary metabolites	67 of 1106	2.67e-67	
vvi01100	Metabolic pathways	71 of 1867	5.02e-59	
vvi00940	Phenylpropanoid biosynthesis	34 of 180	7.98e-47	
vvi01230	Biosynthesis of amino acids	26 of 211	3.92e-31	
vvi00270	Cysteine and methionine metabolism	21 of 96	7.41e-30	
vvi00945	Stilbenoid, diarylheptanoid and gingerol biosynthesis	14 of 37	7.67e-23	
vvi00360	Phenylalanine metabolism	15 of 64	7.52e-22	
vvi00941	Flavonoid biosynthesis	14 of 65	5.12e-20	
vvi00260	Glycine, serine and threonine metabolism	13 of 66	3.22e-18	
vvi00130	Ubiquinone and other terpenoid-quinone biosynthesis	10 of 38	2.72e-15	

Figure 8. Protein–protein interaction network for flower bud vs. flower comparison.

In the protein analysis of the development of the fruits (7 d vs. 50 d), many protein clusters were observed (Figure 9 and Table S6). However, we can highlight the porphyrin and chlorophyll metabolism, biosynthesis of secondary metabolites, photosynthesis or cysteine and methionine metabolism being all of those involved in the early growth of fruit. According to the comparisons between 7 d vs. 120 d or 7 d vs. 160 d, we observed that other physiological mechanisms were involved in the subsequent fruit development including RNA polymerase, pyrimidine and purine metabolism, basal transcription factors or nucleotide excision repair (Figures S11 and S12).

Term ID	Term description	Gene	FDR	
vvi01100	Metabolic pathways	43 of 1867	3.07e-33	
vvi00860	Porphyrin and chlorophyll metabolism	13 of 46	4.33e-22	
vvi01110	Biosynthesis of secondary metabolites	26 of 1106	4.92e-19	
vvi00195	Photosynthesis	8 of 55	7.22e-12	
vvi00531	Glycosaminoglycan degradation	5 of 14	2.07e-09	
vvi00270	Cysteine and methionine metabolism	4 of 96	0.00020	
vvi00906	Carotenoid biosynthesis	3 of 35	0.00020	
vvi00130	Ubiquinone and other terpenoid-quinone biosynthesis	3 of 38	0.00022	
vvi04016	MAPK signaling pathway - plant	4 of 122	0.00034	
vvi00710	Carbon fixation in photosynthetic organisms	3 of 61	0.00066	

Figure 9. Protein–protein interaction network for fruit at 7 vs. 50 days.

4. Discussion

4.1. Refined De Novo Transcriptome Assembly

According to the assembled and refined transcriptome, a total of 142,025 contigs ($\bar{x}$ = 1044 bp, N50 = 1133 bp) were obtained, of which 106,603 contigs corresponded to Trinity "genes" unigenes. Within the assembled contigs, the size ranged from 501 bp to 36,186 bp long. In a similar study assaying *Actinidia eriantha*, the assembly of the filtered reads reached a total of 69,396 unigenes obtaining sizes between 201 and 9602 bp [32]. In comparison with previous studies, our results were of better quality showing a larger number of contigs and size.

On the other hand, regarding the completeness of the ultra-conserved protein evaluation by CEGMA and BUSCO, the obtained scores suggested that the assembled transcriptome contains an important number of ultra-conserved proteins complete or fragmented, indicating the high-quality standard transcriptome in terms of completeness. This biological approach indicated the high-quality score especially for BUSCO which reached almost 70% of the complete genes found in the different datasets. This 70% from the BUSCO score seems to be lower against the quality scores reported above in different plant genomes, but the construction of the de novo transcriptome from three different plant tissues may explain this difference. CEGMA and BUSCO complete scores over 95% were reported for twelve plant genomes including the model plant *Arabidopsis thaliana* and the fruit tree *Pyrus communis* L. var 'Bartlett' [33]. In agreement with these previous results, the sum of the values of the completed and fragmented genes obtained in our study was close to 90%, which was quite high considering the construction of a de novo transcriptome. In addition, a specific tissue de novo transcriptome assembly of *Ilex paraguariensis* [34] obtained similar data with around 73% of complete genes reaching close to 85%.

4.2. Gene Annotation and Enrichment Analysis

In the gene annotation and enrichment analysis, we obtained significant functional annotations from each tissue comparison, including shoot vs. leaf, flower bud vs. flower and for fruit development. In the case of the shoot vs. leaf comparison, the top hits for the biological processes were related to metabolic processes (GO:0008152) or cellular component organization (GO:0071840), while for molecular function it was molecule binding (GO:0005488). Therefore, these processes may be involved in the biosynthesis of constituent macromolecules and plant cells related to leaf development and growth. When we compared bud vs. flower and fruit development (fruit 7 d vs. 50 d–120 d–160 d), the top hit for biological processes was metabolic processes (GO:0008152), while for molecular function the catalytic activity (GO:0003824) was the most significant for both tissue comparisons indicating an increase in the chemical reactions linked to flowering and fruit development.

In addition, only eight GO terms were found for shoot vs. leaf, probably due to the lack of protein annotations related to these tissues. However, flower bud vs. flower and fruit development comparisons showed 119 and 56 GO terms, respectively. Thus, for flower bud vs. flower, some significant protein IDs were related to the anatomical structure development (*p*-value of 6.5e-27; GO:0048856), reproductive process (3.4e-12; GO:0022414), aromatic compound biosynthesis process (7.4e-07; GO:0019438) or response to abiotic stimulus (100e-07; GO:0009628). Therefore, GO:0048856 is related to the progression of anatomical structures including the flower bud to a mature flower. The protein network involved in GO:0022414 was described as responsible for the inheritance of cytoplasmic male sterility in soybeans during flower development [35]. The aromatic compound biosynthesis process (GO:0019438) includes all of the chemical reactions and pathways related to the formation of aromatic compounds which can be happening during flower development, so the aromatic composition of the kiwifruit could be forming during flower development as has been described in *Eucalyptus grandis* floral tissues [36]. For the proteins network related to the response to abiotic stimulus (GO:0009628), recent studies in flower buds from transgenic blueberry evidenced its relation to flower development [37].

Finally, in the case of fruit development (fruit 7 d vs. 50 d–120 d–160 d), some protein IDs were associated with protein metabolic processes (4.1e-3; GO:0019538), DNA polymerase activity (3.9e-10; GO:0034061), transferase activity (6.1e-06; GO:0016740) or catalytic activity (1.6e-03; GO:0003824). In other plant species including cucumber, some of the main proteins linked to fruit development were involved in the process of protein metabolism (GO:0019538) [38]. In addition, some of the most important proteins involved in the fruit development stage in peaches (cell enlargement) were involved in transferase and catalytic activities [39]. Therefore, a major catalysis reaction and an increase in enzymatic activity seem to be more related to fruit development (GO:0034061, GO:0016740 and GO:0003824). A similar approach was implemented in a de novo assembly of the *Persea*

americana cv. 'Hass' (avocado) transcriptome during fruit development where proteins related to fruit oily characteristics were predominant [40].

4.3. Transcriptome Annotation and Differential Expressed Genes

Only 35.6% of the contigs were annotated against the TAIR10 protein database. This low match could be explained by the lack of information in the protein databases, which implies a lower knowledge in the *Actinidia* genus at protein level and explains the interest of this study. Similar results, however, were obtained in other studies in kiwifruit *Actinidia chinensis* var. 'Jinkui', where from the obtained 140,187 unigenes, only 56,912 (39%) were functionally annotated [41]. In addition, Li et al. (2015a) obtained 51,745 unigenes in *Actinidia arguta* and 30,439 matches to known proteins (58%). More recently, an RNA-seq for different fruit tissues was carried out in *Actinidia eriantha*, reaching 69,783 non-redundant unigenes and only 21,730 (30%) were annotated in different protein databases [32].

Several genes specifically involved in protein translation were observed and linked to hypothetical and predicted proteins (Figure 6 and Table S5). The protein ALO19891.1 (UDP-glycosyltransferase 84J2) (*Camellia sinensis*)) overexpressed in the leaf would be an example. As other authors have reported, UDP-glycosyltransferases (UGTs) play an important role in the plant growth and acclimatization to stress conditions [42], which would explain the overexpression of this protein in the leaves. As for the flower bud and flower comparison, XP_010279585.1 (cytokinin dehydrogenase 9-like) (*Nelumbo nucifera*) was overexpressed in the flower. In recent studies, such as that carried out in *Jatropha curcas* [43], the role of cytokinins in flowering development, especially in the pistil, is confirmed. According to fruit development in the comparison between fruit 7 d and fruit 120 d, XP_010924477.1 (probable inositol oxygenase (*Elaeis guineensis*)) increased, which could be related with the ascorbic acid biosynthesis included in a recent work in tomato [44]. In addition, in the present study XP_016207777.1 (calcium-binding protein CML39 (*Arachis ipaensis*)) was up-regulated by the fruit 160 d. Nowadays, there are evidences that the interaction between calcium and phytohormone signals play an important role in fruit development and ripening; however, the mechanisms that are triggered are still unclear [45].

A work with a similar approach has been recently published in *Actinidia chinensis* [46], where the authors combined the transcriptomic studies with an annotated genome. In this study, the authors investigated gene expression patters in different tissues by an electronic fluorescent pictograph (eFP) browser. Thus, they have been able to identify TFs correlated with floral bud and flower development and with fruit development, maturation and ethylene-induced fruit ripening. Therefore, the current work and the mentioned-above both make a great contribution to the plant community especially in *Actinidia chinensis*.

4.4. Protein–Protein Interaction Network

The mechanisms that control flowering development, fruit and senescence are connected and controlled by different genetics context, which are influenced by the environment [47]. Moreover, the reproductive process is the one that happens more suddenly and may be the most environment-dependent, due to the plants that switch from vegetative growth to flower development only when there are favorable environmental conditions [48]. This fact is of great interest, since the continuity of the species depends on it. The plant progression from vegetative growth to reproductive is called, by some authors, floral transition and this process is not only controlled by a single gene but by a complicated gene network [49].

The obtained results in the protein–protein analysis of the comparison between the shoot and leaf showed the great importance of the plant circadian rhythm affecting the kiwi leaf development. The duration of the day is one of the main factors that induces leaf and floral development, and after a lot of effort and meticulous work in the last decades the flowering locus (FT) was identified [50]. Therefore, in this complex context, in order to elucidate some essential pathways and candidate proteins in silico involved in the development plant tissue process such as leaf, flower, and fruit, the dynamics of the PPI

networks through the gene expression profile could be a useful tool [51]. The metabolism and physiology of the majority of organisms are changing between day and night which is traduced in the biological circadian clock [52].

The obtained result through the PPI network seems to indicate that the circadian rhythm is mainly affecting during the leaf development process, although nitrogen and sulfur metabolism were also important pathways involved in this process. Plants requires nitrogen in high amounts in order to produce sugars or organic acids [53], while sulfur metabolism is an event mainly stimulated by photorespiration [54]. This process occurs in the leaf mesophyll in the presence of light and high oxygen concentrations. In this study, photosynthesis is highly significant in the leaf development. In this sense, Abadie et al. [54] indicated that sulfur assimilation is stimulated by photorespiration and excessive photosynthesis could be detrimental to plant cell sulfur nutrition.

The development from flower bud to flower is the most important event occurring in the plant's life and in this context of the floral transition there were many pathways involved, including the gibberellin pathway and environmental conditions such as the light [55]. In our study, in the flower bud vs. flower comparison, some of the most significant clusters were the biosynthesis of secondary metabolites, phenylpropanoid biosynthesis, or cysteine and methionine metabolism. However, we paid special attention to the enzyme mevalonate kinase (VIT_14s0128g00330.t01), which is the only connection between both of the clusters. Mevalonate kinase is an enzyme that catalyzes the phosphorylation of mevalonate to produce mevalonate 5-phosphate, and a Northern blot analysis in *Arabidopsis* showed that this enzyme is accumulated mainly in the roots and inflorescences [56]. Previous studies in *Arabidopsis* pointed out that in the plant cell, the mevalonate or isoprenoid pathway partly leads the biosynthesis of isoprenoids such as gibberellins [25]. Thus, in spite of this enzyme being in silico identified, this could be considered as one of the main enzyme's candidates involved in the interconnection between phenylpropanoid biosynthesis, and cysteine and methionine metabolism.

Finally, regarding fruit development, in the comparison of fruit development (7 vs. 50 days), there were no clearly defined clusters although the most significant pathways were porphyrin and chlorophyll metabolism, biosynthesis of secondary metabolites, photosynthesis, or cysteine and methionine metabolism. Cysteine is a reduced sulfide molecule and is therefore related to the sulfur metabolism mentioned above in the vegetative development of the leaves. Therefore, this molecule plays an important role in redox signaling and it is synthesized through the incorporation of sulfide into O-acetylserine catalyzed by O-acetylserine(thiol)lyase (OASTL), which is present in mitochondria, chloroplasts, and cytosol. In addition, cytosolic sulfide and chloroplastic S-sulfocysteine have been shown to act as signaling molecules by regulating autophagy and protecting photosystems, respectively [57]. Therefore, the result obtained is fully in concordance with the initial stage of fruit development.

In the last steps of fruit development, analyzing the comparisons in fruit development (7 d vs. 120 and 7 vs. 160 d), the most significant events included those related to RNA polymerase, pyrimidine and purine metabolism, basal transcription factors and nucleotide excision repair. RNA polymerases are holoenzymes that contain catalytic and regulatory/non-catalytic subunits involved in template selection, initiation, elongation, transcriptional fidelity, termination, and RNA processing [58,59]. On the other hand, purine and pyrimidine nucleotides played an essential role in the division and elongation of tissues by acting as basic components of DNA in the nucleus and as transcription components [60]. In addition, a basal transcription factor 3 (BTF3) has been reported to play a significant part in the transcriptional regulation linked with eukaryotes growth and development [61], which could be related to the last stages of the fruit development in kiwi fruits.

5. Conclusions

In this study, high-quality tissue-specific de novo transcriptomes were developed identifying the main differentially expressed genes linked to vegetative growth (comparing

shoot vs. leaves), flower (flower bud vs. flower) and fruit development (fruit at 7, 50, 120 and 160 days) in *Actinidia chinensis* var. *deliciosa* cv. ´Hayward' fruits. This information is of special interest in species, such as kiwifruit, with a wide ploidy level variability. The measured metrics and scores of the transcriptome assembly proved to have enough quality to be a putative database of transcripts. In addition, the biological approach for the transcriptome assembly ensures that the assayed transcriptomes have high-quality and an important number of ultra-conserved proteins. Around 35% of the contigs were annotated, although around of 65% of the contigs did not match with any protein, indicating a large number of sequences not associated to the functional annotations. This work has also provided valuable information, identifying 22,962 exclusive genes for all tissue comparisons and allowing the association of identified proteins with different biological processes and molecular functions involved in the development of vegetative and reproductive tissues. UDP-glycosyltransferase 84J2 in the shoot and leaf comparison, cytokinin dehydrogenase 9-like in the flower bud and flower comparison, or inositol oxygenase and calcium-binding protein CML39 in the fruit development, seem to play an important role. In addition, circadian plant rhythm, and sulfur and nitrogen metabolism were identified as main pathways involved in leaf development. Mevalonate kinase was one of the main enzymes involved in the interconnections between phenylpropanoid biosynthesis and cysteine and methionine metabolism in the flower bud vs. flower comparison. On the other hand, porphyrin and chlorophyll metabolism, biosynthesis of secondary metabolites, photosynthesis, or cysteine and methionine metabolism were the most important pathways involved in the first step of fruit development, whereas RNA polymerase, pyrimidine and purine metabolism or basal transcription factors were mainly related to the last fruit development stages. The obtained results provided new tissue-specific information from the transcriptomic and proteomic point of view for further molecular studies in kiwifruit.

Supplementary Materials: The following are available online at https://www.mdpi.com/article/10.3390/agronomy11050919/s1, Figure S1: GO term annotations for cellular function (shoot vs. leaf), Figure S2: GO term annotations for biological process (shoot vs. leaf), Figure S3: GO term annotations for molecular function (shoot vs. leaf), Figure S4: GO term annotations for cellular function (flower bud vs. flower), Figure S5: GO term annotations for biological processes (flower bud vs. flower), Figure S6: GO term annotations for molecular function (flower bud vs. flower), Figure S7: GO term annotations for cellular function (fruit 7 d vs. 50–120–160 d), Figure S8: GO term annotations for biological processes (fruit 7 d vs. 50–120–160 d), Figure S9: GO term annotations for molecular function (fruit 7 d vs. 50–120–160 d), Figure S10: differential expression gene for each tissue and replicate using edgeR for clustering, Figure S11: protein–protein interaction network for fruit at 7 vs. 120 days, Figure S12: protein–protein interaction network for fruit at 7 vs. 160 days, Table S1: summary of raw data stats, Table S2: GO term enrichment using Panther classification system for each plant tissue comparison, Table S3: GO term enrichment using Panther classification system for each plant tissue comparison, Table S4: functional annotations for all contigs and differential gene expression analyses by plant tissue comparison, Table S5: detail of heatmap including the most significant genes for each tissue comparison using a logFC over 2, Table S6: summary of protein–protein interaction network for each tissue comparison by STRING.

Author Contributions: Conceptualization, J.A.S., C.V.-P. and P.M.-G.; data curation, J.A.S. and C.V.-P.; formal analysis, J.A.S., C.V.-P., and P.Z.; funding acquisition, R.I. and C.M.; investigation, J.A.S.; methodology, J.A.S. and C.V.-P.; project administration, C.J.; resources, R.I. and C.M.; supervision, D.R., P.M.-G., R.I. and C.M.; validation, R.I. and C.M.; visualization and writing—original draft, C.V.-P.; visualization and writing—review editing, J.A.S. All authors have read and agreed to the published version of the manuscript.

References

1. Watanabe, K.; Takashi, B.; Shirato, K. Chromosome Numbers in Kiwifruit (*Actinidia deliciosa*) and Related Species. *J. Jpn. Soc. Hortic. Sci.* **1990**, *58*, 835–840. [CrossRef]
2. Hopping, M.E. Flow cytometric analysis of *Actinidia* species. *N. Z. J. Bot.* **1994**, *32*, 85–93. [CrossRef]
3. Ollitrault-Sammarcelli, F.; Legave, J.M.; Michaux-Ferriere, N.; Hirsch, A.M. Use of flow cytometry for rapid determination of ploidy level in the genus *Actinidia. Sci. Hortic.* **1994**, *57*, 303–313. [CrossRef]
4. Huang, H.; Ferguson, A.R. *Actinidia* in China: Natural Diversity, Phylogeographical Evolution, Interspecific Gene Flow and Kiwifruit Cultivar Improvement. *Acta Hortic.* **2007**, *753*, 31–40. [CrossRef]
5. Zuo, L.; Wang, Z.; Fan, Z.; Tian, S.; Liu, J. Evaluation of Antioxidant and Antiproliferative Properties of Three *Actinidia* (*Actinidia kolomikta*, *Actinidia arguta*, *Actinidia chinensis*) extracts in Vitro. *Int. J. Mol. Sci.* **2012**, *13*, 550–568. [CrossRef] [PubMed]
6. Nishiyama, I.; Fukuda, T.; Shimohashi, A.; Oota, T. Sugar and Organic Acid Composition in the Fruit Juice of Different *Actinidia* Varieties). *Food Sci. Technol. Res.* **2008**, *14*, 67–73. [CrossRef]
7. Huang, S.; Ding, J.; Deng, D.; Tang, W.; Sun, H.; Liu, D.; Zhang, L.; Niu, X.; Zhang, X.; Meng, M.; et al. Draft genome of the kiwifruit *Actinidia* chinensis. *Nat. Commun.* **2013**, *4*, 2640. [CrossRef]
8. Pilkington, S.M.; Crowhurst, R.; Hilario, E.; Nardozza, S.; Fraser, L.; Peng, Y.; Gunaseelan, K.; Simpson, R.; Tahir, J.; Deroles, S.C.; et al. A manually annotated *Actinidia* chinensis var. chinensis (kiwifruit) genome highlights the challenges associated with draft genomes and gene prediction in plants. *BMC Genom.* **2018**, *19*, 257. [CrossRef] [PubMed]
9. Tang, W.; Sun, X.; Yue, J.; Tang, X.; Jiao, C.; Yang, Y.; Niu, X.; Miao, M.; Zhang, D.; Huang, S.; et al. Chromosome-scale genome assembly of kiwifruit *Actinidia eriantha* with single-molecule sequencing and chromatin interaction mapping. *Gigascience* **2019**, *8*, giz027. [CrossRef]
10. Wu, H.; Ma, T.; Kang, M.; Ai, F.; Zhang, J.; Dong, G.; Liu, J.A. high-quality *Actinidia chinensis* (kiwifruit) genome. *Hortic. Res.* **2019**, *6*, 117. [CrossRef]
11. Yue, J.; Liu, J.; Tang, W.; Wu, Y.Q.; Tang, X.; Li, W.; Yang, Y.; Wang, L.; Huang, S.; Fang, C.; et al. Kiwifruit Genome Database (KGD): A comprehensive resource for kiwifruit genomics. *Hortic. Res.* **2020**, *7*, 117. [CrossRef]
12. Li, X.; Qin, H.; Wang, Z.; Zhang, Q.; Liu, Y.; Xu, P.; Zhao, Y.; Fan, S.; Yang, Y.; Ai, J. Differentially expressed genes in male and female flower buds of hardy kiwifruit (*Actinidia Arguta* (Sieb. et ZUCC.) Planch. Ex MIQ.). *Bangladesh J. Bot.* **2015**, *44*, 909–915.
13. Tang, W.; Zheng, Y.; Dong, J.; Yu, J.; Yue, J.; Liu, F.; Guo, X.; Huang, S.; Wisniewski, M.; Sun, J.; et al. Comprehensive Transcriptome Profiling Reveals Long Noncoding RNA Expression and Alternative Splicing Regulation during Fruit Development and Ripening in Kiwifruit (*Actinidia chinensis*). *Front. Plant Sci.* **2016**, *7*, 335. [CrossRef]
14. Wu, R.; Wang, T.; Warren, B.A.W.; Allan, A.C.; Macknight, R.C.; Varkonyi-Gasic, E. Kiwifruit SVP2 gene prevents premature budbreak during dormancy. *J. Exp. Bot.* **2017**, *68*, 1071–1082. [CrossRef] [PubMed]
15. Tang, P.; Zhang, Q.; Yao, X. Comparative transcript profiling explores differentially expressed genes associated with sexual phenotype in kiwifruit. *PLoS ONE* **2017**, *12*, e0180542. [CrossRef] [PubMed]
16. Wang, Z.; Liu, Y.; Li, D.; Li, L.; Zhang, Q.; Wang, S.; Huang, H. Identification of Circular RNAs in Kiwifruit and Their Species-Specific Response to Bacterial Canker Pathogen Invasion. *Front. Plant Sci.* **2017**, *8*, 413. [CrossRef] [PubMed]
17. Michelotti, V.; Lamontanara, A.; Buriani, G.; Orrù, L.; Cellini, A.; Donati, I.; Vanneste, J.L.; Cattivelli, L.; Tacconi, G.; Spinelli, F. Comparative transcriptome analysis of the interaction between *Actinidia chinensis* var. *chinensis* and *Pseudomonas syringae pv. actinidiae* in absence and presence of acibenzolar-S-methyl. *BMC Genom.* **2018**, *19*, 585. [CrossRef] [PubMed]
18. Wang, Y.; Xiong, G.; He, Z.; Yan, M.; Zou, M.; Jiang, J. Transcriptome analysis of *Actinidia chinensis* in response to Botryosphaeria dothidea infection. *PLoS ONE* **2020**, *8*, e0227303. [CrossRef]
19. Salazar, J.; Zapata, P.; Silva, C.; González, M.; Pacheco, I.; Bastías, M.; Meneses, C.; Jorquera, C.; Moreno, I.; Shinya, P.; et al. Transcriptome analysis and postharvest behavior of the kiwifruit 'Actinidia deliciosa' reveal the role of ethylene-related phytohormones during fruit ripening. *Tree Genet. Genomes* **2021**, *17*, 8. [CrossRef]

20. Man, Y.P.; Wang, Y.C.; Jiang, Z.W.; Gong, J.J. Transcriptomic analysis of pigmented inner pericarp of red-fleshed kiwifruit in response to high temperature. *Acta Hortic.* **2015**, *1096*, 215–219. [CrossRef]

21. Li, W.; Liu, Y.; Zeng, S.; Xiao, G.; Wang, G.; Wang, Y.; Peng, M.; Huang, H. Gene Expression Profiling of Development and Anthocyanin Accumulation in Kiwifruit (*Actinidia chinensis*) Based on Transcriptome Sequencing. *PLoS ONE* **2015**, *10*, e0136439.

22. Li, Y.; Fang, J.; Qi, X.; Lin, M.; Zhong, Y.; Sun, L. A key structural gene, AaLDOX, is involved in anthocyanin biosynthesis in all red-fleshed kiwifruit (*Actinidia arguta*) based on transcriptome analysis. *Gene* **2018**, *648*, 31–41. [CrossRef] [PubMed]

23. Lin, M.; Fang, J.; Qi, X.; Li, Y.; Chen, J.; Sun, L.; Zhong, Y. iTRAQ-based quantitative proteomic analysis reveals alterations in the metabolism of *Actinidia arguta*. *Sci. Rep.* **2017**, *7*, 5670. [CrossRef]

24. Kim, G.D.; Lee, J.Y.; Auh, J.H. Metabolomic Screening of Anti-Inflammatory Compounds from the Leaves of *Actinidia arguta* (Hardy Kiwi). *Foods* **2019**, *8*, 47. [CrossRef]

25. Kasahara, H.; Hanada, A.; Kuzuyama, T.; Takagi, M.; Kamiya, Y.; Yamaguchi, S. Contribution of the Mevalonate and Methylery-thritol Phosphate Pathways to the Biosynthesis of Gibberellins in Arabidopsis. *J. Biol. Chem.* **2002**, *277*, 45188–45194. [CrossRef]

26. Sponsel, V.M. Signal achievements in gibberellin research: The second half-century. *Annu. Plant Rev.* **2016**, *49*, 1–36.

27. Salinero, M.C.; Vela, P.; Sainz, M.J. Phenological growth stages of kiwifruit (*Actinidia deliciosa* "Hayward"). *Sci. Hortic.* **2009**, *121*, 27–31. [CrossRef]

28. Mi, H.; Muruganujan, A.; Casagrande, J.T.; Thomas, P.D. Large-scale gene function analysis with the PANTHER classification system. *Nat. Protoc.* **2013**, *8*, 1551–1566. [CrossRef]

29. Tian, T.; Liu, Y.; Yan, H.; You, Q.; Yi, X.; Du, Z.; Xu, W.; Su, Z. agriGO v2. 0: A GO analysis toolkit for the agricultural community. *Nucleic Acid Res.* **2017**, *45*, W122–W129. [CrossRef] [PubMed]

30. Szklarczyk, D.; Morris, J.H.; Cook, H.; Kuhn, M.; Wyder, S.; Simonovic, M.; Santos, A.; Doncheva, N.T.; Roth, A.; Bork, P.; et al. The STRING database in 2017: Quality-controlled protein-protein association networks, made broadly accessible. *Nucleic Acids Res.* **2017**, *45*, D362–D368. [CrossRef] [PubMed]

31. Robinson, M.D.; McCarthy, D.J.; Smyth, G.K. edgeR: A Bioconductor package for differential expression analysis of digital gene expression data. *Bioinformatics* **2010**, *26*, 139–140. [CrossRef]

32. Guo, R.; Landis, J.B.; Moore, M.J.; Meng, A.; Jian, S.; Yao, X.; Wang, H. Development and Application of Transcriptome-Derived Microsatellites in *Actinidia eriantha* (Actinidiaceae). *Front. Plant Sci.* **2017**, *8*, 1383. [CrossRef] [PubMed]

33. Veeckman, E.; Ruttink, T.; Vandepoele, K. Are We There Yet? Reliably Estimating the Completeness of Plant Genome Sequences. *Plant Cell* **2016**, *28*, 1759–1768. [CrossRef]

34. Fay, J.V.; Watkins, C.J.; Shrestha, R.K.; Litwiñiuk, S.L.; Talavera Stefani, L.N.; Rojas, C.A.; Argüelles, C.F.; Ferreras, J.A.; Caccamo, M.; Miretti, M.M. Yerba mate (*Ilex paraguariensis*, A. St.-Hil.) de novo transcriptome assembly based on tissue specific genomic expression profiles. *BMC Genom.* **2018**, *19*, 891. [CrossRef]

35. Chen, L.; Ding, X.; Zhang, H.; He, T.; Li, Y.; Wang, T.; Li, X.; Jin, L.; Song, Q.; Yang, S.; et al. Comparative analysis of circular RNAs between soybean cytoplasmic male-sterile line NJCMS1A and its maintainer NJCMS1B by high-throughput sequencing. *BMC Genom.* **2018**, *19*, 663. [CrossRef]

36. Vining, K.J.; Romanel, E.; Jones, R.C.; Klocko, A.; Alves-Ferreira, M.; Hefer, C.A.; Amarasinghe, V.; Dharmawardhana, P.; Naithani, S.; Ranik, M.; et al. The floral transcriptome of *Eucalyptus grandis*. *New Phytol.* **2014**, *206*, 1406–1422. [CrossRef]

37. Song, G.Q.; Gao, X. Transcriptomic changes reveal gene networks responding to the overexpression of a blueberry DWARF AND DELAYED FLOWERING 1 gene in transgenic blueberry plants. *BMC Plant Biol.* **2017**, *17*, 106. [CrossRef] [PubMed]

38. Li, J.; Xu, J.; Guo, Q.W.; Wu, Z.; Zhang, T.; Zhang, K.J.; Cheng, C.Y.; Zhu, P.Y.; Lou, Q.F.; Chen, J.F. Proteomic insight into fruit set of cucumber (*Cucumis sativus* L.) suggests the cues of hormone-independent parthenocarpy. *BMC Genom.* **2017**, *18*, 896. [CrossRef]

39. Guidarelli, M.; Zubini, P.; Nanni, V.; Bonghi, C.; Rasori, A.; Bertolini, P.; Baraldi, E. Gene expression analysis of peach fruit at different growth stages and with different susceptibility to *Monilinia laxa*. *Eur. J. Plant Pathol.* **2014**, *140*, 503–513. [CrossRef]

40. Vergara-Pulgar, C.; Rothkegel, K.; González-Agüero, M.; Pedreschi, R.; Campos-Vargas, R.; Defilippi, B.G.; Meneses, C. *De novo* assembly of *Persea americana* cv. "Hass" transcriptome during fruit development. *BMC Genom.* **2019**, *20*, 108. [CrossRef] [PubMed]

41. Zhang, J.Y.; Huang, S.N.; Mo, Z.H.; Xuan, J.P.; Jia, X.D.; Wang, G.; Guo, Z.R. *De novo* transcriptome sequencing and comparative analysis of differentially expressed genes in kiwifruit under waterlogging stress. *Mol. Breed.* **2015**, *35*, 208. [CrossRef]

42. Zhang, Z.; Zhuo, X.; Yan, X.; Zhang, Q. Comparative Genomic and Transcriptomic Analyses of Family-1 UDP Glycosyltransferase in *Prunus Mume*. *Int. J. Mol. Sci.* **2018**, *19*, 3382. [CrossRef] [PubMed]

43. Ming, X.; Tao, Y.-B.; Fu, Q.; Tang, M.; He, H.; Chen, M.S.; Pan, B.Z.; Xu, Z.F. Flower-Specific Overproduction of Cytokinins Altered Flower Development and Sex Expression in the Perennial Woody Plant *Jatropha curcas* L. *Int. J. Mol. Sci.* **2020**, *21*, 640. [CrossRef]

44. Munir, S.; Mumtaz, M.A.; Ahiakpa, J.K.; Liu, G.; Chen, W.; Zhou, G.; Zheng, W.; Ye, Z.; Zhang, Y. Genome-wide analysis of Myo-inositol oxygenase gene family in tomato reveals their involvement in ascorbic acid accumulation. *BMC Genom.* **2020**, *21*, 284. [CrossRef] [PubMed]

45. Gao, Q.; Xiong, T.; Li, X.; Chen, W.; Zhu, X. Calcium and calcium sensors in fruit development and ripening. *Sci. Hortic.* **2019**, *253*, 412–421. [CrossRef]

46. Brian, L.; Warren, B.; McAtee, P.; Rodrigues, J.; Nieuwenhuizen, N.; Pasha, A.; David, K.M.; Richardson, A.; Provart, N.J.; Allan, A.C.; et al. A gene expression atlas for kiwifruit (*Actinidia chinensis*) and network analysis of transcription factors. *BMC Plant Biol.* **2021**, *21*, 121. [CrossRef]

47. Huijser, P.; Schmid, M. The control of developmental phase transitions in plants. *Development* **2011**, *138*, 4117–4129. [CrossRef] [PubMed]

48. Baurle, I.; Dean, C. The timing of developmental transitions in plants. *Cell* **2006**, *125*, 655–664. [CrossRef] [PubMed]

49. He, F.; Zhou, Y.; Zhang, Z. Deciphering the *Arabidopsis* floral transition process by integrating a protein-protein interaction network and gene expression data. *Plant Physiol.* **2010**, *153*, 1492–1505. [CrossRef]

50. Turck, F.; Fornara, F.; Coupland, G. Regulation and identity of florigen: FLOWERING LOCUS T moves center stage. *Annu. Rev. Plant Biol.* **2008**, *59*, 573–594. [CrossRef]

51. Han, J.D.; Bertin, N.; Hao, T.; Goldberg, D.S.; Berriz, G.F.; Zhang, L.V.; Dupuy, D.; Walhout, A.J.; Cusick, M.E.; Roth, F.P.; et al. Evidence for dynamically organized modularity in the yeast protein-protein interaction network. *Nature* **2004**, *430*, 88–93. [CrossRef]

52. McClung, C.R. Plant Circadian Rhythms. *Plant Cell* **2006**, *18*, 792–803. [CrossRef]

53. Nunes-Nesi, A.; Fernie, A.R.; Stitt, M. Metabolic and Signaling Aspects Underpinning the Regulation of Plant Carbon Nitrogen Interactions. *Mol. Plant* **2010**, *3*, 973–996. [CrossRef]

54. Abadie, C.; Tcherkez, G. Plant sulphur metabolism is stimulated by photorespiration. *Commun. Biol.* **2019**, *2*, 379. [CrossRef] [PubMed]

55. Henderson, I.R.; Dean, C. Control of *Arabidopsis* flowering: The chill before the bloom. *Development* **2004**, *131*, 3829–3838. [CrossRef]

56. Lluch, M.A.; Masferrer, A.; Arró, M.; Boronat, A.; Ferrer, A. Molecular cloning and expression analysis of the mevalonate kinase gene from *Arabidopsis thaliana*. *Plant Mol. Biol.* **2000**, *42*, 365–376. [CrossRef]

57. Romero, L.C.; Aroca, M.A.; Laureano-Marín, A.M.; Moreno, I.; García, I.; Gotor, C. Cysteine and Cysteine-Related Signaling Pathways in *Arabidopsis thaliana*. *Mol. Plant* **2014**, *7*, 264–276. [CrossRef] [PubMed]

58. Werner, F.; Grohmann, D. Evolution of multisubunit RNA polymerases in the three domains of life. *Nat. Rev. Microbiol.* **2011**, *9*, 85–98. [CrossRef]

59. Cramer, P.; Armache, K.J.; Baumli, S.; Benkert, S.; Brueckner, F.; Buchen, C.; Damsma, G.E.; Dengl, S.; Geiger, S.R.; Jasiak, A.J.; et al. Structure of eukaryotic RNA polymerases. *Annu. Rev. Biophys.* **2008**, *37*, 337–352. [CrossRef]

60. Zrenner, R.; Stitt, M.; Sonnewald, U.; Boldt, R. Pyrimidine and purine biosynthesis and degradation in plants. *Annu. Rev. Plant Biol.* **2006**, *57*, 805–836. [CrossRef] [PubMed]

61. Jamil, M.; Wang, W.; Xu, M.; Tu, J. Exploring the roles of basal transcription factor 3 in eukaryotic growth and development. *Biotechnol. Genet. Eng. Rev.* **2015**, *31*, 21–45. [CrossRef] [PubMed]